ORIGINAL ARTICLE

Endovenous laser coagulation: asymmetrical heat transfer and coagulation (modeling in blood plasma)

Vladimir P. Minaev[1] · Nikita V. Minaev[2] · Vadim Yu Bogachev[3] · Konstantin A. Kaperiz[4] · Vladimir I. Yusupov[2]

Abstract

The objective of this study was to describe the dynamics of blood plasma heating and coagulation processes carried out by continuous laser radiation with wavelengths 1.55 and 1.94 μm through bare-tip fibers and fibers with radial output (radial fibers) used for endovenous laser coagulation (EVLC). The study was performed in previously thawed frozen donor blood plasma using high-speed shooting of the heating process through the shadow optical method. It has been shown that in the case of highly water-absorbed laser radiations, convection, explosive, and small-bubble boiling play a major role in the process of heat transfer and coagulation. It has been shown that in the case of radiation with wavelength λ = 1.94 μm, effective heat transfer begins at significantly lower levels of power compared to radiations with λ = 1.55 μm. It has been established that heat transfer is sharply asymmetrical and is directed mainly upwards and forwards (bare-tip fiber) or upwards (radial fibers). For a wavelength of 1.94 μm, the effect of self-cleaning of the fiber surface from coagulated plasma fragments was found. Except for short-term acts of explosive boiling, the heat transfer is asymmetrical and directed mainly upwards. This effect should lead to uneven heating and thermal damage to the vein wall with the maximum at its upper part. For EVLC, the use of radiation with a wavelength of 1.94 μm is more efficient and safer.

Keywords Bare-tip fibers · Radial fibers · blood plasma · "Water-absorbing" range · Convection · Explosive boiling · Coagulation · Self-cleaning · EVLT · EVLA · EVLC

✉ Nikita V. Minaev
  minaevn@gmail.com

1 NTO IRE-Polus, pl. Akad, Vvedenskogo 1, stroenie 3, 141190 Fryazino, Moscow region, Russia

2 Institute of Photon Technologies, Federal Scientific Research Centre «Crystallography and Photonics», Russian Academy of Sciences, Pionerskaya ul. 2, 108840, Moscow Troitsk, Russia

3 Pirogov Russian National Research Medical University, Ostrovityanova str.1, 117997 Moscow, Russia

4 "The First Phlebological Center", Dmitriya Ul'yanova 31, 117447 Moscow, Russia

Introduction

Endovenous laser coagulation (EVLC) has become more and more popular in clinical practice for the treatment of varicose veins due to low invasiveness and high effectiveness, as well as the easy adoption of this approach by doctors. It is generally accepted that the main process triggering the fibrous transformation of the vein exposed to EVLC is the vein wall thermal damage [1]. The choice of optimal wavelengths of laser radiation, exposure modes, and ways of radiation output from optic fibers remains debatable.

In order to get an answer to this question, mathematical modeling was carried out (e.g. , [2–4] of the thermal processes taking place at EVLC in the vein). However, in mathematical modeling, there is always a question of the correctness of the selected model. In addition, it turns out to be problematic to check the results and conclusions obtained during this mathematical modeling.

In this regard, issues of physical modeling of the processes taking place during EVLC remain relevant. Because of the

opacity of the blood, the dynamics of the changes in density inhomogeneities (bubbles and areas of protein coagulation) in the process in veins with blood can be studied only by ultrasound registration methods. However, the obtained sonograms do not allow for unambiguous interpretation.

Optical registration methods can give more comprehensive information. The work [5] describes the use of a water solution of surface-active substance and blood serum for modeling heat transfer processes under laser radiation with wavelengths of 0.97 and 1.47 μm. The authors concluded that foaming of suspension of denaturized blood proteins caused by boiling played an important role in the coagulation of vein contents under laser heating. The sonograms obtained from EVLC and laser obliteration of cysts are also interpreted from this point of view. At the same time, there is no detailed analysis of heat transfer to the vein wall providing its thermal damage. In addition, the study did not cover the use of 1.94-μm-length radiation, which has been recently considered the most promising for EVLC [6–9].

This work was carried out after the work [10], which compared the results of heat transfer in water when heated by laser radiation with wavelengths of 1.47, 1.55, and 1.94 μm using optic fibers for EVLC. There were used for the experiment's bare fiber, and fibers with radiation output approximately perpendicular to the fiber axis through the ring apertures at 360° on its side surface ("radial" fibers).

Figure 1 shows from [11] dependence on wavelength of absorption coefficients in water and erythrocyte emulsion, simulating blood with hematocrit Hct = 33.2% and effective attenuation coefficient estimated in [12], taking into account scattering in blood besides absorption.

Since absorption in water is higher than absorption in hemoglobin for radiation with these wavelengths, the processes in water can simulate heat transfer in blood in the first approximation. It was shown that depending on radiation power and
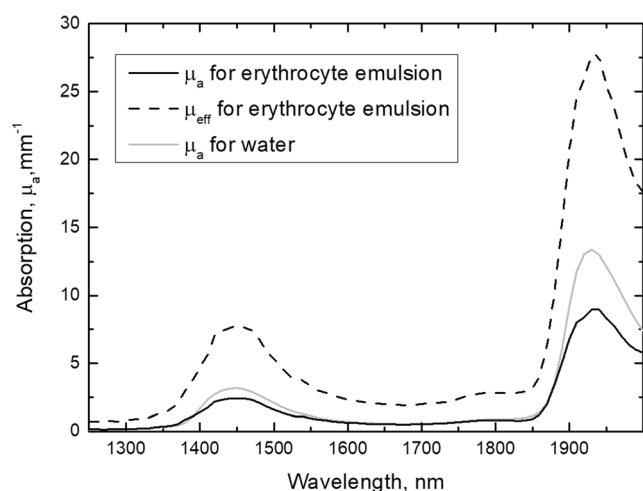

Fig. 1 Absorption μ_a and effective attenuation μ_{eff} in erythrocyte emulsion (model of blood with hematocrit Hct = 33,2%) and absorption μa in water

wavelength, heat transfer is carried out through convection, bubble, or explosive boiling. The investigation results have shown that thermal transfer in a stream of heated suspension and vapor-gas bubbles that transfer heat occurs mainly asymmetrically, forward-upwards for the bare fibers, and upwards for the radial fibers. At the same time, it is difficult to predict how significant blood viscosity and coagulation will affect the processes occurring in blood.

A more suitable object for modeling heat transfer processes during laser heating of blood is blood plasma, which is closer in composition to the blood and contains a number of coagulating proteins, such as fibrinogen and antihemophilic globulin, that were absent in blood serum used in the work [5]. In addition, blood and plasma possess similar characteristics of laser radiation absorption, and the transparency of plasma allows the use of optical registration methods.

This paper presents the results of the heat transfer and coagulation process investigation that occur under heating by laser radiation with wavelengths of 1.55 and 1.94 μm in blood plasma. The detected significant asymmetry of the heat transfer process will inevitably lead to asymmetric heating of the vein wall and, therefore, uneven thermal damage during EVLC.

Materials and methods

Laser devices LSP-"IRE-Polyus" (CW, radiation wavelength λ = 1.55 μm, maximum output power Pmax = 15 W and λ = 1.94 μm, Pmax = 10 W) were used as radiation sources. The same experimental installations are used for experiments as in the work [10] (Fig. 2a). Plasma was poured into a rectangular cuvette 1 with a size of 25 × 35 × 110 mm. A shell from the introducer 6F (Balton, Poland) with the valve 3 was used to insert and fix the fibers 2 in the cuvette. The experiments were carried out at room temperature 23 ± 1 °C.

Transparent cuvette walls allowed surveying the area near the fiber outlet end, which was carried out perpendicular to the fiber axis ("side face", camera 4) and along the axis ("full face", speed camera 5). Shadow pictures were taken with a high-speed camera Fastcam SA3 (Photron, USA) at a speed of 4000 frames per second (250 μs between frames), frame duration 20 μs, using background illumination through the cuvette. This high-speed shooting mode allowed for clear, blur-free shots. In addition, ordinary images in scattered light were taken with a digital camera XCAM1080PHB (ToupTek, China) full HD (1920 × 1080) at 30 frames per second. In some experiments, the high-speed camera was in position 4, and shadow pictures were taken side face.

A high-speed camera was used to record the displacements of density inhomogeneities and the refractive index of the medium. This made it possible to observe the formation and movement of vapor-gas bubbles, zones of coagulation, and
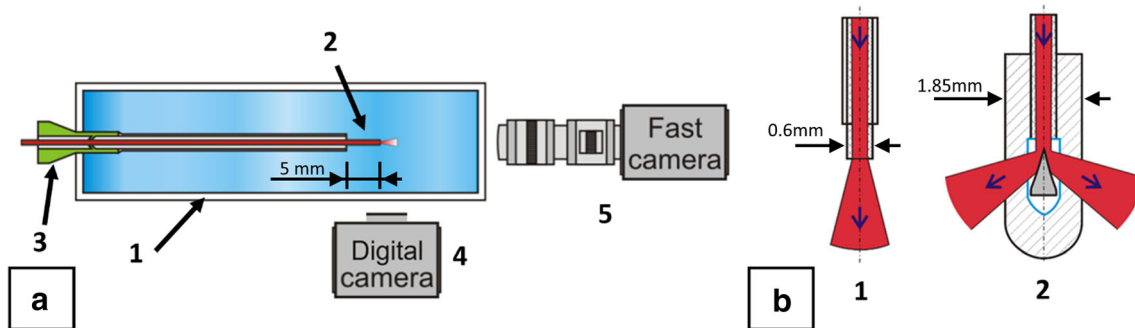
Fig. 2 a Installation scheme: 1, cuvette with blood plasma; 2, fiber; 3, introducer for the fiber; 4, digital camera for shooting "side face"; 5, high-speed camera for shooting full face; b, scheme of laser radiation output from the bare-tip (1) and radial (2) fibers

carbonization in liquid media. In addition, the movement of thermal fronts was measured – sharp boundaries separating the heated region of the suspension of coagulated plasma particles and the unheated region. The boundaries between the regions were visible due to the large gradient of the refractive index, which depends on the temperature.

Temperature benchmarks that estimate the value of temperature are plasma protein coagulation (60–70 °C), water boiling (≥ 100 °C), and carbonation (> 150 °C) [13–15].

Bare fibers were quartz-quartz; core has diameter 0.6 mm and was made of water free quartz. Fiber with radial output was produced by Biolitec AG (Germany). The diameter of the protective flask of the radial fibers was 1.85 mm. A schematic image of the radiation output from optic fibers is presented in Fig. 2b. Before each experiment, we additionally checked the presence of axial symmetry and a uniform propagation pattern for all optical fibers used in the experiments using a pilot laser beam in the visible range.

The optic fibers were not moved in all the experiments.

The study was performed in frozen donor blood plasma from the bank of blood, which was previously thawed by standard medical procedure.

The experiment used the following parameters of laser exposure—optic fibers with bare-tip: $\lambda = 1.55$ μm $P = 5$; 7 and 10 W; $\lambda = 1.94$ μm $P = 1$; 2; 5 and 7 W, and optic fiber with radial output: $\lambda = 1.55$ μm $P = 8$ and 10 W; $\lambda = 1.94$ μm $P = 2$ and 5 W.

Experimental results and discussion

Bare-tip optic fiber

Wavelength $\lambda = 1.55$ μm

Figure 3 presents the results of the side face shooting of the processes occurring when blood plasma is heated by laser radiation with a wavelength of 1.55 μm and power $P = 5$ W. The radiation is supplied through a fiber with a diameter of 0.6 mm with end radiation output (bare fiber).

After laser radiation $\lambda = 1.55$ μm is switched on, the blood plasma is gradually heated in a distance of about $L = 1$ (Fig. 3a) mm from the fiber end. This is evidenced by the appearance of a dark horizontal area at the upper edge of the fiber in the shadow picture (frame 0.01 s in Fig. 3a) caused by a gradient of the refraction index due to uneven heating of the plasma. At the same time, there are no changes in digital pictures taken in scattered light (frame 0.01 s in Fig. 3b). After that, the coagulation of the heated plasma begins, the area with which is clearly manifested in the shadow picture and the picture in scattered light (frame 0.03 s in Fig. 3a, b). At the same time, an upward laminar convective flow is formed, which carries away heated suspension of the coagulated plasma components. The flow width of about 1.3 mm is well visible in shadow and ordinary pictures. The heatwave front speed is about 10 mm/s, which is approximately 1.5 times less than under similar conditions in water. This is a consequence of higher viscosity of blood plasma compared to water.

This process continues for approximately 2 s, after which an act of explosive boiling lasting less than 0.1 s occurs near the fiber end (frame 2.066 s in Fig. 3c). Then, the picture of laminar convective heat transfer is restored again (frame 2.2 s in Fig. 3c).

After about 4 s from the radiation switching on, a clot of coagulated plasma begins to form at the upper edge of the fiber (Fig. 3d). The lower edge of the clot falls down along the end, blocking the output of convective heat and suspension of coagulated particles flow. Because of this, the flow is forced to bend the clot; an overheated area is formed at the fiber end due to the lack of effective convective cooling in the coagulation area. This results in another act of explosive boiling at 10 s. After explosive boiling, the particles stuck on the fiber end are partially charred and heated up to high temperatures causing glowing at the fiber end (frame 10.1 s in Fig. 3d).

As a result, a coagulate with numerous bubbles smaller than the optic fiber diameter (Fig. 3e) is formed at 15 s near the fiber end around the heated area, through which steam-gas bubbles rush upwards. At 30 s, a bright shining appears in coagulate near the optic fiber end, and at the same time, the formation of steam-gas bubbles and convective streams accelerates. The authors think that in this case, due to overheating, the organic
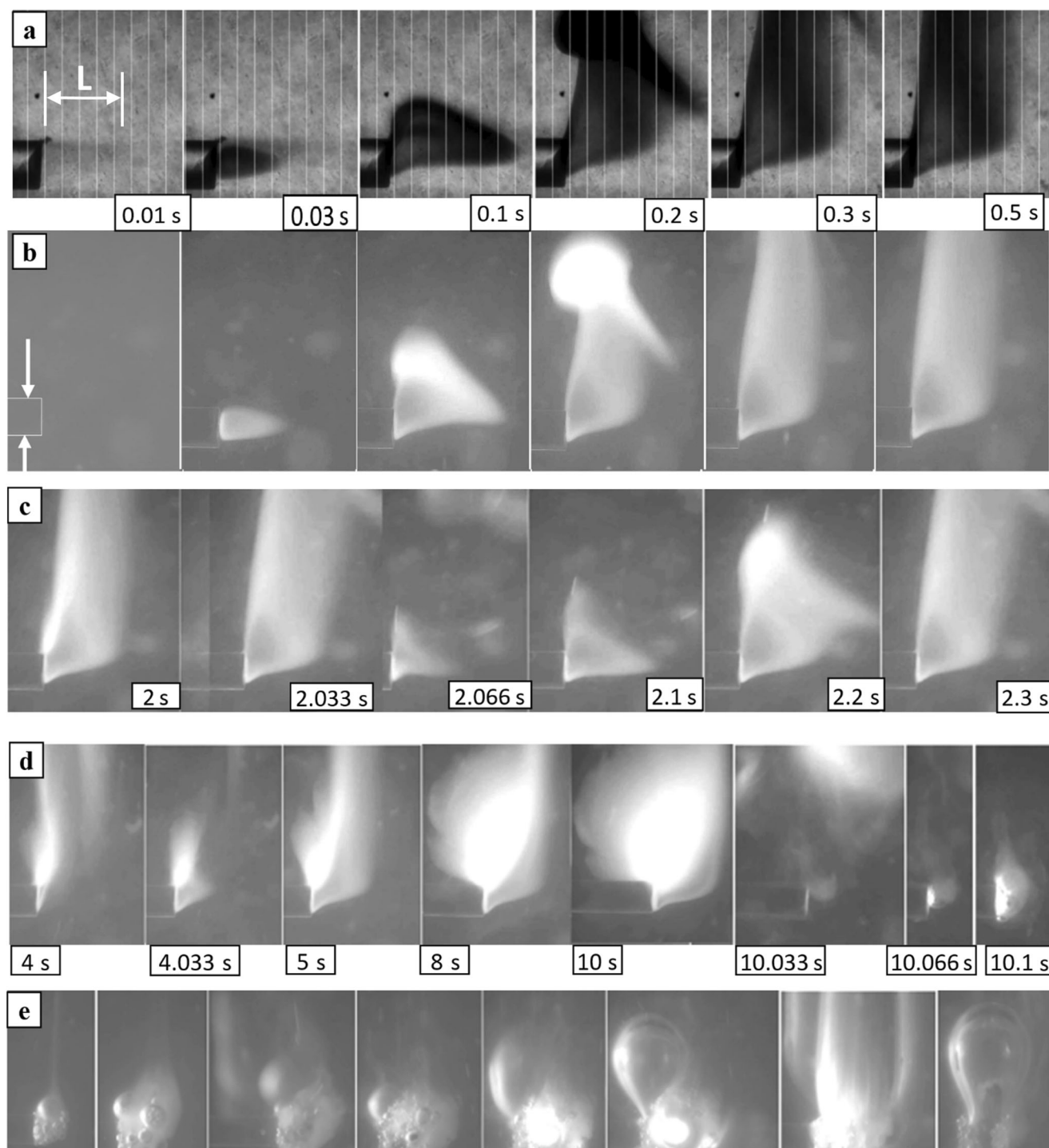
Fig. 3 Dynamics of heat transfer and coagulation of blood plasma when heated with radiation $\lambda = 1.55$ μm, $P = 5$ W: (**a**) high-speed shooting of the shadow picture (the distance between vertical strips is 0.19 mm); (**b**–**e**) images from the digital camera in scattered light. The numbers show the time from the moment when radiation was switched on, arrows in Fig. 2b mark the diameter of the fiber (0.6 mm)

component of the coagulate has again been charred, what has led to a sharp increase in the absorption rate of laser radiation, accompanied by a strong increase in temperature. The rapid growth of the bubbles is explained by the release of gases dissolved in the liquid due to strong heating. In addition, since plasma proteins consist mainly of carbon, it can be assumed that

as a result of combustion (frame 30.033 s in Fig. 3e), CO and CO_2 will be released. Frame 31 s in Fig. 3e corresponds to the moment when radiation is switched off. One can see the charred tissue sticking to the optic fiber end in the picture.

It should be noted that charring and heating of the fiber end up to high temperatures are undesirable, because in this case,

contact with the vein wall can cause its perforation leading to complications in the form of ecchymosis and hematomas [15].

A similar pattern is observed at higher power levels ($P = 7$ and 10 W), but all processes are expected to occur faster. Figure 4a presents a shadow picture of the processes during the first 0.5 s at $P = 7$ W. At the same time, the vertical speed of the heatwave front is about 13 mm/s at $P = 7$ W and ≈ 15 mm/s at $P = 10$ W. The width of the convective flow reaches approximately 1.3 mm at $P = 7$ W and 1.6 mm at $P = 10$ W.

The figures show the time from the moment when radiation was switched on; the arrows in Fig. 4b indicate the fiber diameter (0.6 mm). The digital pictures obtained in scattered light show that the area containing bubbles and coagulated plasma is gradually increasing at $P = 7$ W after a period of laminar convective flow and start of bubble boiling at the fiber end, which can be seen (frame 4 s in Fig. 4b). Then, part of the coagulate is charred due to high temperature, which leads to the rapid heating of the area near the fiber end up to the shining temperature (frame 4.66 s in Fig. 4b). At the same time, the size of the bubbles increases, apparently, due to the release of carbon dioxide as a result of organics combustion. After radiation switching off at 5 s, the gas bubble remains at the fiber end and charred tissue is visible (frame 7 s in Fig. 4b).

Thus, the experiments show that the following processes occur when blood plasma is exposed to laser radiation with $\lambda = 1.55$ μm and power within $P = 3$–10 W through the bare fiber. In the first moments after the radiation was switched on, a laminar convective flow of coagulated particles suspension was formed in heated plasma, directed upwards. This process was interrupted by a short-term (within 1–3 ms) act of explosive boiling, resulting in the spreading of the heated plasma with steam-gas microbubbles and particles of coagulated plasma in all directions.

Then, the convective flow can recover, or a clot of coagulated blood plasma is formed at the optic fiber end. Bubble boiling occurs inside this clot causing the upward flow of heated coagulated particles suspension. At some point in time, the radiation absorption rate increased dramatically due to charring of organic components, accumulated near the fiber end, causing this area to heat up to the shining temperature. At the same time, carbon dioxide formed by burning organics was added to the steam and gases which were previously dissolved in blood plasma. This is evidenced by the increased volume of bubbles that remains unchanged after the radiation was switched off (after steam condensation) and the presence of charred tissue on the optic fiber end.

Thus, except for short-term moments of explosive boiling, heat transfer resulting from exposure to laser radiation goes mainly upwards.

Wavelength $\lambda = 1.94$ μm

Processes are different in the case of laser radiation with wavelength $\lambda = 1.94$ μm. Since radiation with $\lambda = 1.94$ μm is more absorbed in the water, and therefore in blood plasma, the width of the area in which radiation is absorbed is much smaller (no more than $L = 0.2$ mm). The stage of convective heat transfer is observed after the activation of radiation only at low
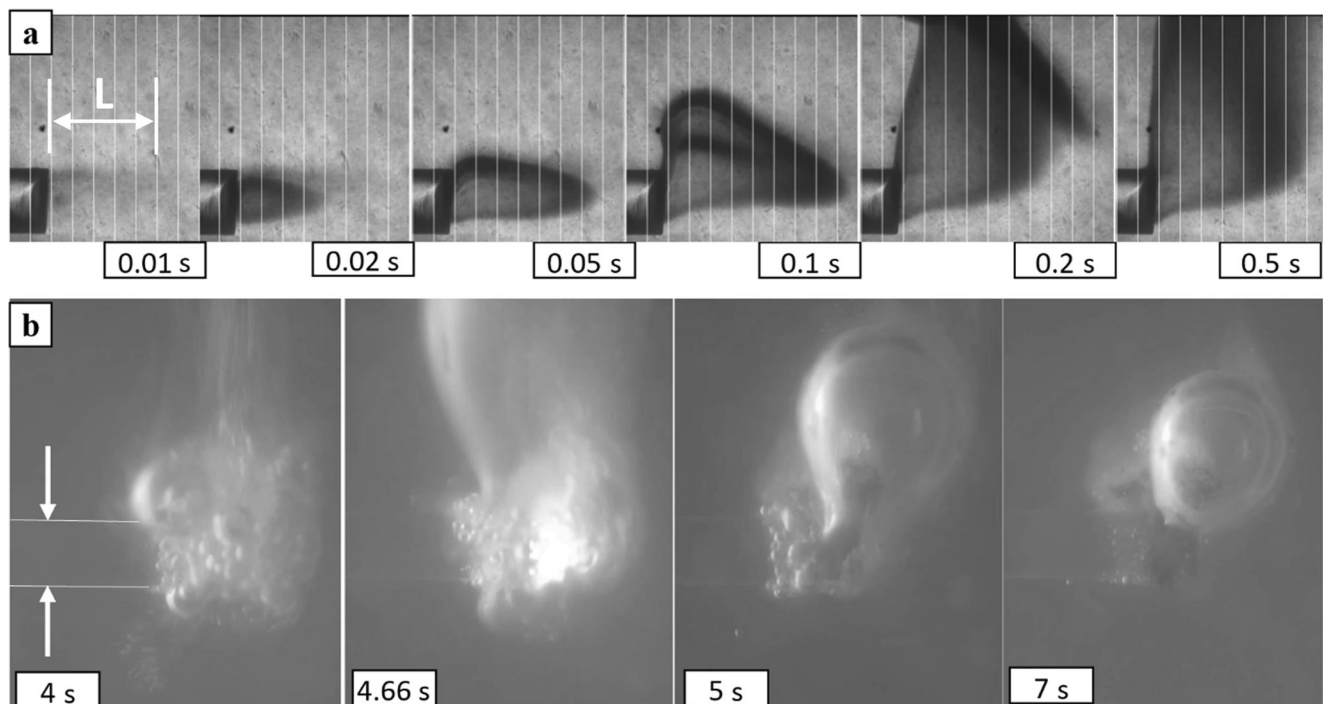

Fig. 4 Pictures of plasma heat transfer and plasma coagulation when heated by radiation $\lambda = 1.55$ μm, $P = 7$ W: (**a**) high-speed shooting of a shadow picture (the distance between vertical stripes is 0.19 mm); (**b**) digital images in scattered light

power levels. Convective flows do not have time to develop before explosive boiling already at radiation power $P = 1$ W (Fig. 5) due to the thin radiation absorption area at the fiber end (frame 32.5 s in Fig. 5a).

As in the case of experiments with water [10], 0.5-ms explosive boiling releases a cloud of steam-gas microbubbles (frame 32.75 ms, Fig. 5a) and heated liquid expanding forward (in this case at a speed of about 3.5 m/s) and slightly to the sides.

Because of explosive boiling, the end was cleaned and remains clean for about 2 ms. Then, the area of heated liquid (frame 37 ms, Fig. 5a) began to re-form at the optic fiber end. Steam-gas bubbles were formed inside this area. It can be assumed that since bubbles actively absorb various nano-micro-inclusions [16] from the liquid on their interface, their walls will consist of fragments of coagulated plasma. When this gradually increasing highly heterogeneous area (Fig. 5a)

completely closes the fiber end at 66 ms, an explosion occurs spreading microbubbles and heated suspension of the coagulated plasma particles. The speed of spreading was about 0.36 m/s, which is an order of magnitude less than in the first act of explosive boiling.

Then, a gas bubble began to grow at the fiber end. At the same time, radiation passed through bubble contents (Moses effect [17]), and convective suspension flow with particles of coagulated plasma was formed at bubbles distal end. The flow began to move upwards (Fig. 5b).

At 645 ms, overheating of near-wall fluid of the bubble caused another act of explosive boiling (Fig. 5b), which created an expanding cloud of steam-gas bubbles and heated suspension of the coagulated plasma particles, and the base of convective flow is destroyed. At the same time, the spreading speed varied from about 1.5 m/s in 1 mm at the fiber end to about 0.38 m/s in 3 mm from it.
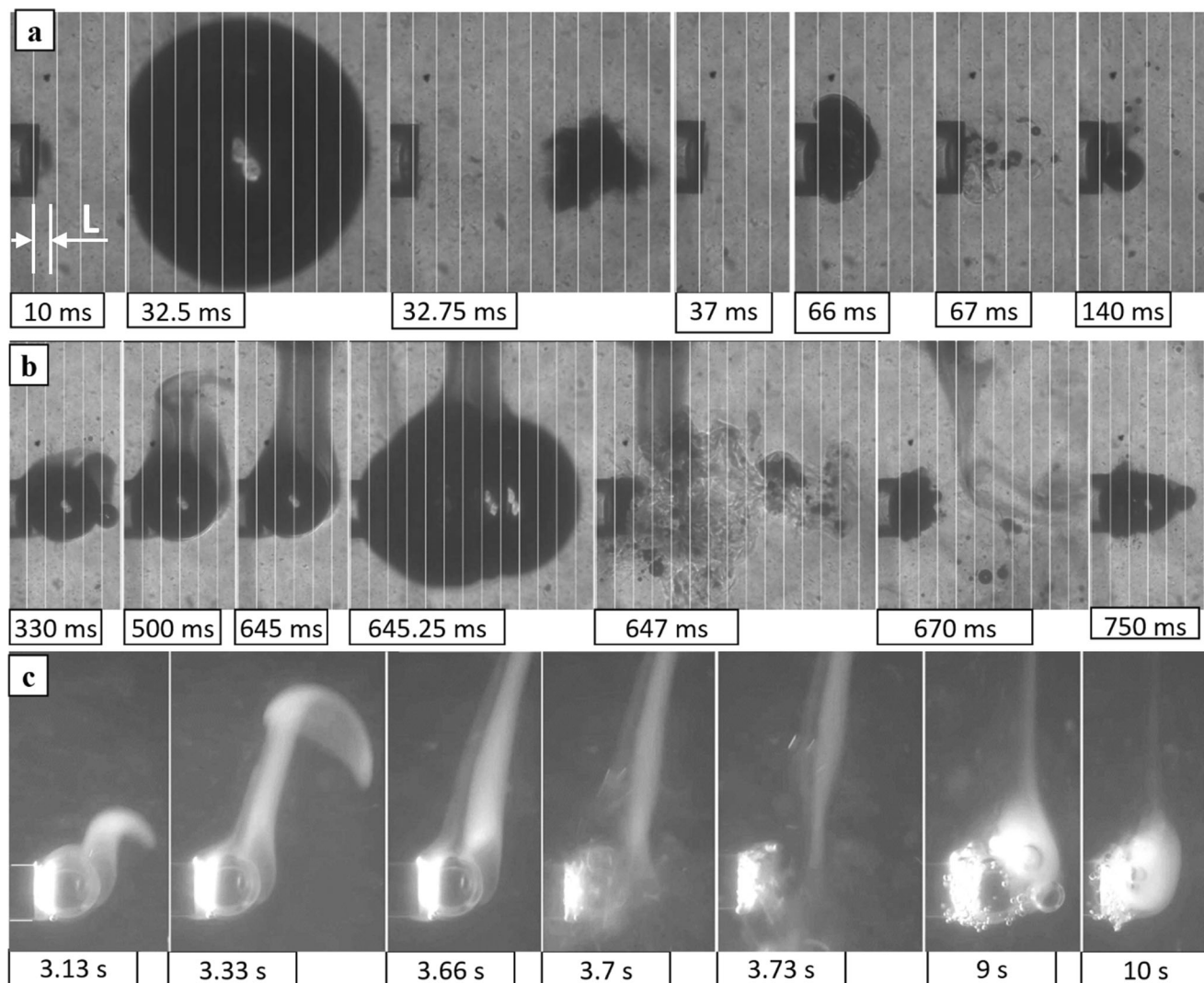

Fig. 5 Pictures of heat transfer in blood plasma when heated with radiation $\lambda = 1.94$ μm, $P = 1$ W: (a, b) high-speed shooting of the shadow picture. The distance between vertical stripes is 0.19 mm; (c) digital picture in scattered light. The numbers show the time from the moment, when radiation was switched on

Then, a steam-gas bubble began to re-form near the fiber end (frames 670 and 750 ms in Fig. 5b).

Further development of the process is presented in digital pictures in scattered light (Fig. 5c). The convective flow of heated suspension of coagulated plasma particles began to form at the bubble surface near the fiber end, and then, it spreads upwards. The front speed was approximately 6 mm/s. At some point (frame 3.7 s in Fig. 5c), the bubble explodes due to overheating of near-wall fluid (the act of explosive boiling) resulting in the destruction of the convective flow base and spreading of heated liquid, steam-gas microbubbles, and particles of coagulated plasma. At the same time, the fiber end is partially cleaned from surrounding particles. In subsequent moments, a steam-gas bubble was re-formed at the fiber end (and remains until the next explosion). A clot of coagulated plasma is formed on its surface containing small steam-gas bubbles. Low-intensity convective flow moved upwards from this clot. After radiation is deactivated (frame 10 s in Fig. 5c), steam-gas bubbles greatly shrink in size due to the condensation of steam. They contain almost only gas previously dissolved in liquid. As a result, a clot of coagulated blood plasma remained on the fiber end.

Figure 6 presents the results of the processes registration that occur when plasma is heated through the bare fiber by laser light with $\lambda = 1.94$ μm at radiation power $P = 5$ W.

As with lower power, there is no convective heat transfer at the initial stage. After 3 ms, an act of explosive boiling occurred in the thin layer near the fiber end as a result of plasma overheating. A steam-gas bubble was formed. As in the case of power $P = 1$ W, the bubble collapses and a cloud of steam-gas microbubbles and heated plasma was released forward with a speed of about 3.8 m/s, slightly expanding to the sides. At the same time, the end of fiber was completely cleaned.

Then, once radiation continues, the plasma began to boil at the fiber end with the formation and collapse of bubbles, the diameter of which was smaller than the diameter of the fiber. At the same time, the speed of the flow formed due to boiling was about 0.35 m/s. Acts of explosive boiling occur periodically; their duration did not exceed 1 ms. A high-speed camera recorded 11 acts of explosive boiling in total (during 0.4 s of shooting).

Shooting in scattered light with a digital camera has shown that a rarefied flow of coagulated plasma suspension directed mainly forward (Fig. 6c) was observed within view during 6.5 s. It spreads flakes of coagulated plasma throughout the cuvette. The formation of upward convective laminar flows recorded at radiation power 1 W (Fig. 5) was not observed in this case. A glowing area with a thickness of about 0.1 mm was observed during the entire exposure to laser radiation at the fiber end. However, after radiation was switched off, the fiber end remained clean (frame 6.5 s in Fig. 6c). That is, particles do not stick to the fiber end due to intense boiling at $P = 5$ W. Similar results were obtained in the power range $P = 2$–7 W.

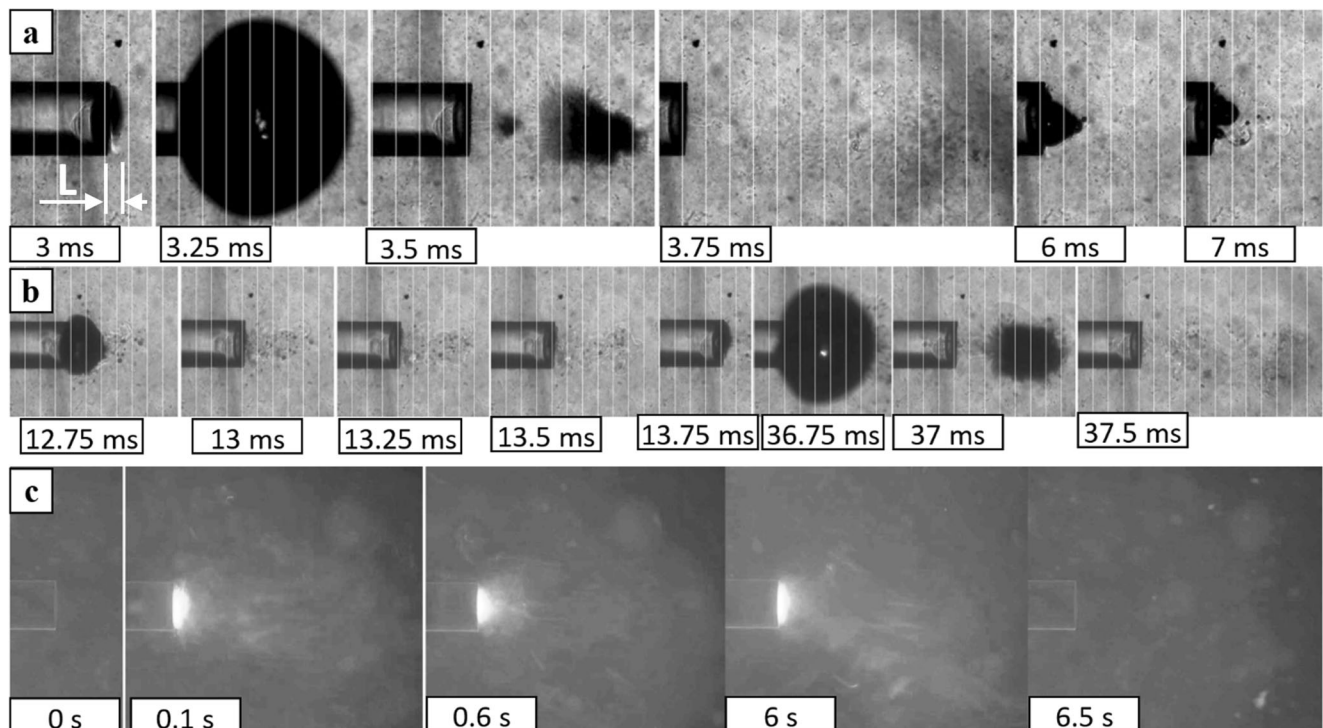**Fig. 6** Pictures of heat transfer in blood plasma when heated with radiation $\lambda = 1.94$ μm, $P = 5$ W: (**a**, **b**) high-speed shooting of the shadow picture. The distance between vertical stripes is 0.19 mm; (**c**) digital picture in scattered light. The numbers show the time from the moment when radiation was switched on

The experiments have shown that when blood plasma was heated with radiation $\lambda = 1.94$ μm through the bare-tip fibers, the processes of effective heat transport and coagulation begin at lower power levels and proceed more intensively compared to these processes at $\lambda = 1.55$ μm. At the same time, starting with power $P = 2$ W, there is no laminar convective heat transfer at the initial stage.

Exposure to radiation emitted through the fiber end results in a forward-directed flow of heated suspension, coagulated particles of blood plasma and steam-gas microbubbles that are formed due to explosive and bubble boiling.

In the power range $P = 2$–7 W, the fiber end is cleaned; that is, no conglomerates of coagulated blood plasma are formed at the fiber end, leading to charring and heating of the fiber end up to shining temperature.

Fiber with radial output

Wavelength $\lambda = 1.55$ μm

The aperture area estimated using the pictures [10], through which the radiation is guided from the used radial optic fiber with a protective flask diameter of 1.85 mm, by 6 ± 1 times exceeds the output aperture of the bare fiber with a diameter of 0.6 mm. Therefore, the EVLC procedure with a radial fiber is usually carried out at higher power levels. In particular, typical power values used in the First Phlebological Center (Moscow, Russia) for the medical EVLC procedure are $P = 8$–10 W for $\lambda = 1.55$ μm and $P = 4$–5 W for $\lambda = 1.94$ μm.

Figure 7 shows the results of the optical registration of the impact of laser radiation with $\lambda = 1.55$ μm at $P = 7$ W on blood plasma. Registration is carried out simultaneously full face (towards the fiber axis) through the shadow method using a high-speed camera (Fig. 7a) and side face (perpendicular to the optic fiber axis) in scattered light using a digital camera (Fig. 7b–d).

One can see in the presented frames that the convective flow of heated liquid is formed after the plasma is heated with laser radiation near the fiber. The flow is directed upward and contains flakes of coagulated blood plasma. This flow created a narrow "channel" with a width equal to the width of the radiating aperture. It is clearly visible in scattered light pictures (Fig. 7b). The speed of the convective flow front was about 13 mm/s.

This pattern remained for about 4 s. Figure 7c presents frames at 4.3 s after switching on of radiation recorded side face by a digital camera in scattered light. At this point, an area consisting of clumped flakes of coagulated plasma was formed near the upper wall of the protective flask of the optic fiber. It limited the spreading of the heat flow (frame 4.3 s in Fig. 7c). As a result, the content of this area was overheated, which led to an explosive boiling (frame 4.33 s in Fig. 6c). Because of this, the formed area and convective flow were destroyed, and streams of heated liquid and flakes of coagulated plasma spread in different directions.

After the act of explosive boiling, a ring of coagulated plasma remained on the protective flask of the light guide near the radiation output. As a result, the nature of the further process significantly changed (Fig. 7d). The process entered the stage of "small-bubble boiling", resulting in a clot of coagulated plasma around the flask, in which water from blood plasma boiled with the release of heated liquid and flakes of coagulated plasma. As a result, both heat and all heated suspension moved upwards, partly in the form of laminar heat flow. At the same time, self-cleaning of the flask from sticking coagulated plasma particles did not occur, and the next act of explosive boiling can be expected in time. After radiation was switched off (12.1 s in Fig. 7d), the volume of bubbles in the clot quickly decreased due to steam condensation. It results in a clot of coagulated plasma with bubbles formed by gases previously dissolved in plasma, which is formed on the optic fiber after 14 s.

Thus, the heat flow was directed upwards except for the moment of explosive boiling.

Wavelength $\lambda = 1.94$ μm

In the case of radiation with $\lambda = 1.94$ μm, the process of effective heat transfer began at lower power levels than in the case of $\lambda = 1.55$ μm. Figure 8 shows the results of optical registration of the impact of laser radiation through the radial optic fiber with power $P = 5$ W on blood plasma. Registration is carried out simultaneously full face through the shadow method using a high-speed camera (Fig. 8a) and side face in scattered light using a digital camera (Fig. 7c, d).

After the activation of radiation, a laminar convective channel was being formed during the first 0.39 s. Heated suspension of coagulated plasma particles was carried upwards through this channel. The speed of flow front spreading was about 8 mm/s.

There is an act of intense explosive boiling at 393 ms, lasting less than 1 ms, which destroyed laminar convective flow (Fig. 8 a, b). At the same time, flows of heated suspension with particles of coagulated plasma were spread in all directions.

After that, small-bubble boiling began near the protective flask of the optic fiber. It was accompanied by the formation of turbulent flows of heated plasma and coagulate flakes spreading mainly upwards.

One should note that in this case, liquid near the optic fiber surface was not much overheated, and there are no acts of explosive boiling leading to periodical complete cleaning of the optic fiber. At the same time, there was a noticeable cleaning of the flask surface from the sticking coagulate in the process of small-bubble boiling. The amount of this coagulate was significantly lower than
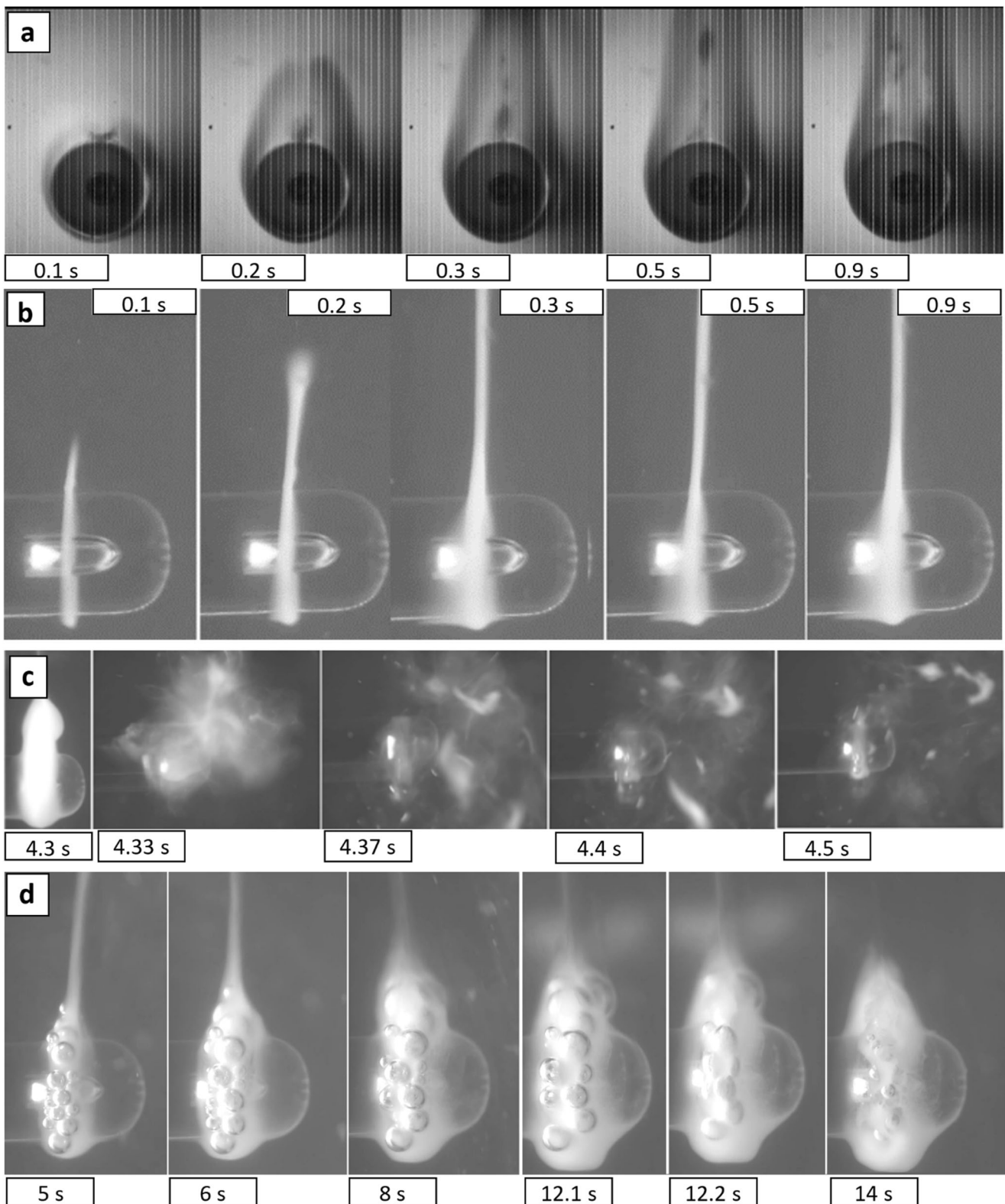
Fig. 7 Dynamics of heat transfer and coagulation of blood plasma when heated with radiation λ = 1.55 μm, P = 10 W, "radial" fiber: (**a**) high-speed shooting of a shadow picture full face, (**b–d**) shooting with a digital camera side face in scattered light. The numbers show the time elapsed after radiation was switched on

in the case of radiation with λ = 1.55 μm and power P = 10 W. Conditions for formation of a conglomerate of coagulated particles with sizes sufficient to start carbonation are not created.

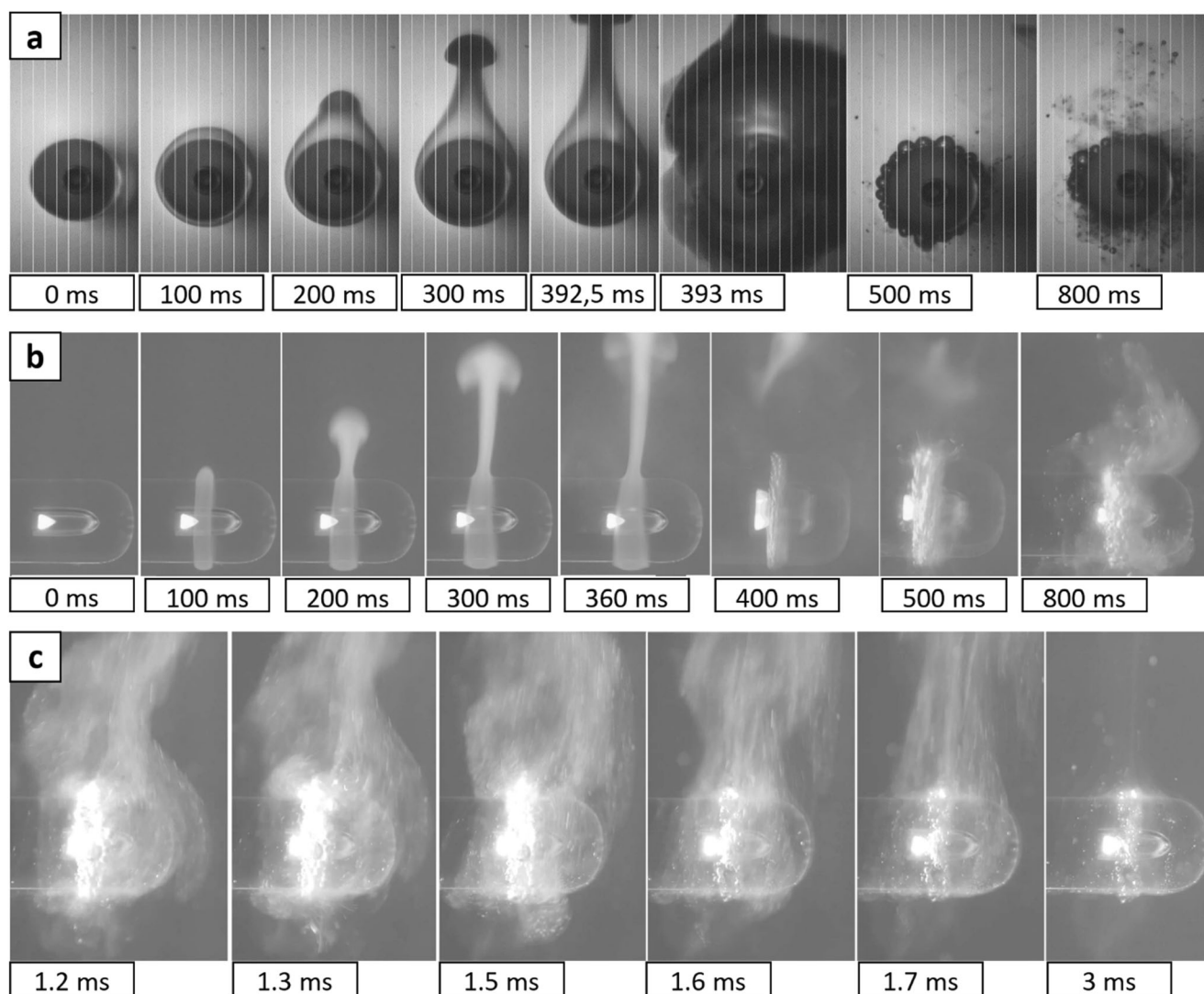**Fig. 8** Dynamics of heat transfer and coagulation of blood plasma when heated with radiation λ = 1.94 μm, P = 5 W, "radial" optic fiber: (**a**) high-speed shooting of a shadow picture full face, (**b**) shooting side face with a digital camera in scattered light. The numbers show the time elapsed after radiation was switched on

It should be noted that similar processes are observed at radiation λ = 1.94 μm and P = 2 W, but the intensity of bubble boiling is not enough to clean the optic fiber from the conglomerate of coagulated plasma which was formed at the radiation output.

Results of experiments show that for both bare fibers and fibers with radial output except for short-term acts of explosive boiling, the heat transfer is asymmetrical and directed mainly upwards. This means that the symmetric consideration used in [2–4] does not correspond to real processes of heat transfer.

How does heat transfer occur in the vein during EVLC?

The experiments described in this work were carried out with almost unlimited liquid. Let us consider how the processes of heat transfer take place during EVLC, when blood is limited by the vein walls. Immediately after the laser light is switched on, a blood clot overlaps the vein at the beginning of the EVLC, so almost the entire procedure occurs in the absence of blood flow. The experiments have shown that when blood in vein is heated with laser radiation that is strongly absorbed in water, the heat transfer, except for short-term moments of explosive boiling, occurs in the upward direction; i.e., heat transfer in the vein will be directed to its upper wall (Fig. 9).

Streams heated suspension of the coagulated plasma particles and steam-gas bubbles reach the upper vein wall and begin to spread along it in all directions. Since heated streams move along the wall and transfer heat to it, their temperature should fall. Therefore, the further from the contact area is, the lower degree of heating of the vein wall is. Its thermal damage necessary to start the process of fibrous transformation is also

Fig. 9 Distribution diagram for heat-carrying flows during EVLC: a bare fiber, side face view; b cross-section; c radial fiber, full-face view. 1 vein wall, 2 optic fiber for laser radiation, 3 blood. The dashed red arrows show the direction of heated suspension flows
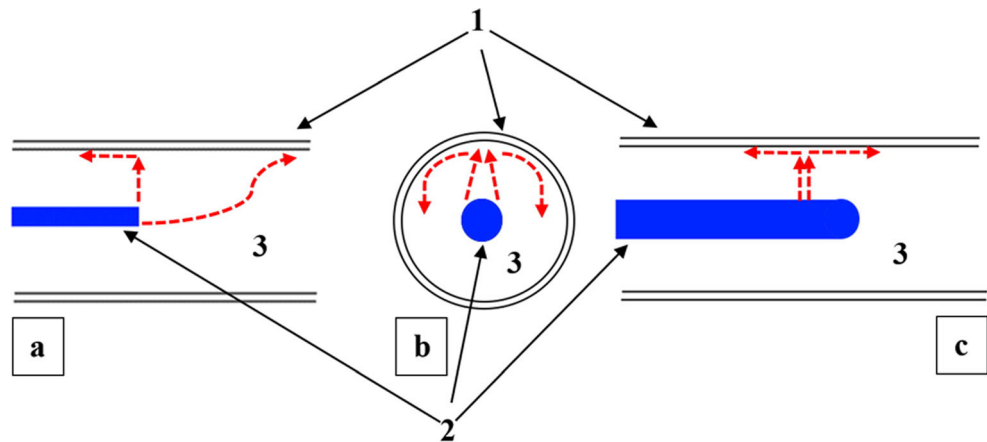
lower. In this case, particles of coagulated blood will fill the vein opening from top to bottom. Thus, the results of the experiments suggest that EVLC is characterized by uneven thermal damage to the vein wall with the maximum at its upper part.

We explain the greater effectiveness of 1.94 μm by the possibility of carrying out treatment at about 2 times lower powers compared to 1.55 μm. Due to the detected self-cleaning effect using radiation of 1.94 μm, the probability of carbonization and associated heating of the end of the fiber to high temperatures is less. Heating the end of the fiber can lead to perforations of the vein wall and related complications (ecchymosis, hematomas).

Experiments in the cuvette have shown that effective heat transfer at 1.94 μm is achieved at lower power levels compared to 1.55 μm and that it is less likely that the end of the light guide will warm up due to carbonation of the coagulate near it.

Conclusions

The processes of heat transfer and coagulation of blood plasma have been studied under exposure to laser radiation with wavelengths λ = 1.55 μm and λ = 1.94 μm through radial and bare fibers, which are used for the treatment of varicose veins.

The experiments have shown that, as with water [10], effective thermal transfer begins at lower power levels for radiation with λ = 1.94 μm compared to radiation with λ = 1.55 μm.

In the case of bare-tip optic fiber with end radiation output, λ = 1.55 μm and power up to P = 10 W, the main role in the process of heat transfer belongs to laminar convection, explosive, and small-bubble boiling. These processes are accompanied by plasma coagulation, with coagulated plasma flakes being carried away by heated fluid flows. The flow of heated suspension of the coagulated plasma particles spreads sharply asymmetrically and is directed mainly upwards most of the

time. A clot of coagulated plasma particles accumulates over time at the optic fiber end. Carbonation occurs in this clot, increasing the absorption of laser radiation avalanche-like, which leads to the heating of carbonized tissue up to shining temperature. Contact between the optic fiber and the vein wall can cause wall perforation leading to complications in the form of ecchymosis and hematomas.

In the case of the bare fiber with λ = 1.94 μm, starting with the power of P = 2 W, the stage of laminar convective heat transfer is absent, and boiling at the optic fiber end causes the formation of a forward-directed flow of heated suspension of coagulated plasma particles. This suspension subsequently moves upward.

For radiation with λ = 1.94 μm and power over P = 2 W, the effect of cleaning the optic fiber end from sticking organic particles has been found. In this case, carbonized tissue on the optic fiber is not formed, and its unwanted heating does not occur.

Using radial optic fiber with radiation λ = 1.55 μm and power P = 7–10 W, as well as radiation λ = 1.94 μm and power P = 2–5 W, results in the formation of upward-directed laminar flows of heated coagulated plasma particles at the initial stage. This process is subsequently replaced by acts of explosive boiling and small-bubble boiling. In the case of radiation λ = 1.55 μm, the formation of a conglomerate of coagulated plasma particles is observed near the radiation output area, whereas in the case of radiation λ = 1.94 μm, there is a noticeable self-cleaning of the optic fiber due to intense bubble boiling. Thus, it can be assumed that an increase in the power of radiation with λ = 1.94 μm with a simultaneous increase in the speed of optic fiber traction during the medical procedure is a rather promising approach. This will not only improve the efficiency of self-cleaning of the optic fiber preventing unwanted carbonation but also reduce operation time.

The detected effect of optic fiber self-cleaning explains the fact that there is almost no carbonation of the optic fiber end when using laser radiation with λ = 1.94 μm for clinical

EVLC procedures, while it occurs quite often when using radiation with λ = 1.55 μm. The co-authors of this article, who are practicing phlebologists, in the course of their clinical practice, have established that the frequency of carbonization of the working part of the extracted fiber when using radiation λ = 1.94 μm is much lower than when using λ = 1.55 μm and λ = 1.47 μm and, therefore, more than λ = 0.97 μm.

Experiments show that except for short-term acts of explosive boiling, the heat transfer is asymmetrical and directed mainly upwards. This effect should lead to uneven heating and thermal damage to the vein wall with the maximum at its upper part.

References

1. Proebstle TM, Lehr HA, Kargl A, Espinola-Klein C, Rother W, Bethge S et al (2002) Endovenous treatment of the greater saphenous vein with a 940-nm diode laser: thrombotic occlusion after endoluminal thermal damage by laser-generated steam bubbles. J Vasc Surg 35:729–736. https://doi.org/10.1067/mva.2002.121132

2. Mordon SR, Wassmer B, Zemmouri J (2007) Mathematical modeling of 980-nm and 1320-nm endovenous laser treatment. Lasers Surg Med 39:256–265. https://doi.org/10.1002/lsm.20476

3. Poluektova AA, Malskat WSJ, van Gemert MJC, Vuylsteke ME, Bruijninckx CMA, Martino Neumann HA, van der Geld CWM (2014) Some controversies in endovenous laser ablation of varicose veins addressed by optical–thermal mathematical modeling. Lasers Med Sci 29:441–452. https://doi.org/10.1007/s10103-013-1450-y

4. Artemov S, Belyaev A, Bushukina O, Khrushchalina S, Kostin S, Lyapin A, Ryabochkina P, Taratynova A (2019) Endovenous laser coagulation using two-micron laser radiation: mathematical modeling and in vivo experiments. Advanced Laser Technologies, Prague, Czech Republic 10.24411/9999-011A-2019-00154

5. Chudnovskii VM, Maior AY, Yusupov VI, Zhukov SA (2019) Laser-induced boiling of biological fluids. High Temp 57:531–538. https://doi.org/10.1134/S0018151X19040035

6. Somunyudan MF, Topaloglu N Ergenoglu MU, Gulsoy M. (2011) Endovenous laser ablation with TM-fiber laser Proc of SPIE 7897: 789707-1. https://doi.org/10.1117/12.875411.

7. Belyaev AN, Chabushkin AN, Khrushchalina SA, Kuznetsova OA, Lyapin AA, Romanov KN, Ryabochkina PA (2016) Investigation of endovenous laser ablation of varicose veins in vitro using 1.885-μm laser radiation. Lasers Med Sci 31:503–510. https://doi.org/10.1007/s10103-016-1877-z

8. Mendes-Pinto D, Bastianetto P, Cavalcanti Braga Lyra L, Kikuchi R, Kabnick L (2016) Endovenous laser ablation of the great saphenous vein comparing 1920-nm and 1470-nm diode laser. Int Angiol 35:599–604 http://www.ncbi.nlm.nih.gov/pubmed/26418143

9. Schmedt C-G, Esipova A, Dikic S, Setia A, Demhasaj S, Dieckmann T et al (2016) Endovenous laser therapy (ELT) of saphenous vein reflux using thulium laser (Tm, 1940 nm) with radial fiber – one year results. Eur J Vasc Endovasc Surg 52:413–414. https://doi.org/10.1016/j.ejvs.2016.07.071

10. Minaev VP, Minaev NV, Bogachev VY, Kaperiz KA, Yusupov VI (2020) Endovenous laser coagulation: asymmetrical heat transfer (modeling in water). Lasers Med Sci. https://doi.org/10.1007/s10103-020-03184-y

11. Friebel M, Helfmann J, Netz U, Meinke M (2009) Influence of oxygen saturation on the optical scattering properties of human red blood cells in the spectral range 250 to 2000 nm. J Biomed Opt 14(3):034001

12. Marchenko AA, Minaev VP, Smirnov IV, Shevelkina ED Evaluation of blood optical properties in the wavelength range of 1.3–2.0 μm. Lasernaya Medicina 23(2):44–51 [In Russ.]

13. Tuchin VV (2016) Tissue optics and photonics: light-tissue interaction II. J Biomed Photonics Eng 2(3):030201. https://doi.org/10.18287/JBPE16.02.030201

14. Müller GJ, Sliney DH, Potter RF (1989) Dosimetry of laser radiation in medicine and biology. Society of Photo-Optical Instrumentation Engineers (SPIE) Conference Series. 10305. https://doi.org/10.1117/12.2283582

15. Zhilin KM, Minaev VP, Sokolov AL (2009) Effect of laser radiation absorption in water and blood on the optimal wavelength for endovenous obliteration of varicose veins. Quantum Electron 39: 781–784. https://doi.org/10.1070/QE2009v039n08ABEH014071

16. Yusupov VI, Tsypina SI, Bagratashvili VN (2014) Trapping of nanoparticles in a liquid by laser-induced microbubbles. Laser Phys Lett 11:116001. https://doi.org/10.1088/1612-2011/11/11/116001

17. Elhilali MM, Badaan S, Ibrahim A, Andonian S (2017) Use of the Moses technology to improve holmium laser lithotripsy outcomes: a preclinical study. J Endourol 31:598–604. https://doi.org/10.1089/end.2017.0050